Development of an Open-Source, Discrete Element Knee Model

2 authors:

Anne Schmitz
University of Wisconsin - Stout
72 PUBLICATIONS   **951** CITATIONS

D. Piovesan
Gannon University
159 PUBLICATIONS   **682** CITATIONS

Development of an Open-Source, Discrete Element Knee Model

Anne Schmitz* and Davide Piovesan

Abstract—*Objective*: Biomechanical modeling is an important tool in that it can provide estimates of forces that cannot easily be measured (e.g., soft tissue loads). The goal of this study was to develop a discrete element model of the knee that is open source to allow for utilization of modeling by a wider audience of researchers. *Methods*: A six degree-of-freedom tibiofemoral and one degree-of-freedom patellofemoral joint were created in OpenSim. Eighteen ligament bundles and tibiofemoral contact were included in the model. *Results*: During a passive flexion movement, maximum deviation of the model from the literature occurred at the most flexed angle with deviations of 2° adduction, 7° internal rotation, 1-mm posterior translation, 12-mm inferior translation, and 4-mm lateral translation. Similarly, the overall elongation of the ligaments agreed with literature values with strains of less than 13%. *Conclusion*: These results provide validation of the physiological relevance of the model. *Significance*: This model is one of the few open source, discrete element knee models to date, and has many potential applications, one being for use in an open-source cosimulation framework.

Index Terms—Computational knee model, contact, ligaments, OpenSim, validated knee model.

I. INTRODUCTION

THE knee is the most frequently injured joint, resulting in over 55 million doctor visits a year [1]. Osteoarthritis, the most common form of arthritis, occurs more in the knee than any other joint [2]. Therefore, knee models are valuable tools that can be used to study normal joint function, simulate potential strategies to prevent injury, and assess the effect of treatment programs.

These models range in complexity from a hinge joint [3], [4] to a complex continuum representation using finite element analysis [5]. Uses of these models include the estimation of forces that are difficult to measure (i.e., muscle forces and soft tissue loads) and the performance of "what-if" studies. For example, a simplified joint model has been used to study how muscle weakness affected normal walking [6]. A discrete element model of the knee, which includes cartilage loads and spring representations for ligaments, has been used to predict hamstring and quadriceps forces that could be used to restore normal joint function in a knee without an anterior cruciate ligament (ACL)

[7]. A finite element model of the knee has been utilized to determine how quadriceps forces affect patellofemoral cartilage loads, often the cause of patellofemoral pain [8].

When estimating internal knee loads during movement, it is important to couple musculoskeletal dynamics and soft tissue mechanics (i.e., cosimulation, [9]). Musculoskeletal dynamics include rigid body dynamics and the force-length-velocity behavior of muscles while tissue mechanics encompasses the stress-strain behavior of cartilage and ligaments. Therefore, cosimulation requires a discrete or finite element knee model. This cosimulation approach has been implemented to determine neuromuscular coordination patterns to optimize jumping [10]; to simultaneously predict muscle and contact forces at the knee during gait [11]; and to predict ligament forces during movement [12]. Also, a detailed knee joint model has also been used to calculate cartilage contact loads in a dynamic knee simulator, utilizing a cosimulation technique to simultaneously calculate arthrokinematics and minimize quadriceps loading [13]. Notably, the annual "Grand Challenge Competition to Predict In Vivo Knee Loads" developed by Fregly *et al.*, [14], [15] has also led to many advances in validating these cosimulation approaches to calculate soft tissue loads. For example, Thelen *et al.*, were one of the few groups to include ligaments in the cosimulation framework [16]. This approach led to model predictions of cartilage loads within 4–17% of the experimentally measured values. However, widespread utilization of the cosimulation method is hampered by the time-intensive process of developing and validating a detailed joint model. Open-source models provide a way to make cosimulation more accessible.

Kinematic and finite element open-source models have been developed for the knee joint. For example, a lower-limb musculoskeletal model has been presented in [17] allowing for detailed analyses of the force and torque generating capacities of muscles. However, this model used a simplified, kinematic representation of the knee joint that cannot predict ligament and cartilage contact loads, and hence renders it unsuitable for cosimulation. An open-source, finite element knee model has been developed in [18]. Due to their complexity, though, finite element models can be computationally expensive. On the other hand, discrete element models offer a balance between simplified and finite element models by providing soft tissue loads at a low computational cost. These types of models have been used to investigate how muscles, ligaments, and the ground reaction force contribute to cartilage contact loads [19]. Another recent, notable study developed an open-source knee model with ligaments, three-dimensional (3-D) rotations, and 3-D translations to investigate the effect of nonsagittal movements on ligament function [20]. However, this model did not include cartilage contact forces between the bones. The addition of the

mechanical properties of cartilage allows for the calculation of contact forces between the femur and tibia when multiple contacts points are present. With more than three points of contact, the problem would be ill-posed by simply using a static analysis. Unfortunately, there are very few open-source, discrete element knee models available in the literature.

One reason for the paucity of open-source, discrete element knee models containing both ligaments and contact loads is that researchers develop these models in various software packages (e.g., Matlab, SIMM, C language). This makes reproducing the model and sharing difficult because these packages can be costly. OpenSim [21] is a software package that has been developed in an effort to provide a platform for researchers to share models, components, and analyses. However, validating the model once it has been shared remains difficult. Models are difficult to validate because model components come from different sources: generic bony geometry based on cadavers, muscle and ligament attachments established using the anatomical landmarks, articular geometry of the femur from MRI data of a single specimen, etc.

These two barriers, sharing and validation, can hinder the forward progression of the modeling field. For a researcher to incorporate modeling into a study, extensive time must be spent developing and validating the model. Forward progress can be accelerated if the researcher has a model available to start with. Therefore, the goal of this study was to develop a discrete element model of the knee that is open source for later use in an open-source cosimulation framework for gait. To be utilized in a cosimulation methodology, the model must include both ligaments and cartilage contact. In the following sections, a description of the components constituting the model and the validation process on cadaveric data is described.

II. METHODS

The developed model is available from https://simtk.org/home/kneemodel/ and can be freely downloaded and recreated using OpenSim (version 3.0.1 VC10P [21]).

A. Model Coordinate Systems

The right femur and tibia of a generic musculoskeletal model (i.e., gait2392 model [22]–[25]) were scaled for a 77.5-kg female in the open-source software OpenSim. Collected in a prior study [26], retroreflective markers placed on the greater trochanters, femoral epicondyles, tibial plateaus, and malleoli were used to scale the subject. The origin of the femur coordinate system was placed at the center of the femoral head with the x-axis pointing anteriorly, the y-axis superiorly, and the z-axis to the right (see Fig. 1) [22], [27]. The y-axis was oriented along a line connecting the femoral head and the center of the femoral condyles. The tibial coordinate system was located at the midpoint of the femoral condyles with the knee in full extension. The tibial axes were oriented similarly to the femur coordinate system with the x-axis pointing anteriorly, the y-axis superiorly, and the z-axis to the right [22], [27]. The body fixed coordinate system for the patella was placed at the distal pole of the patella with the x-axis pointing anteriorly, the y-axis superiorly, and the z-axis to

the right (see Fig. 1) [22], [27]. A six degree-of-freedom (dof) tibiofemoral joint and one dof patellofemoral joint were created that included tibiofemoral contact, ligaments, and vastii muscles (see Fig. 1).

B. Patellofemoral Joint

Similar to other models in the literature [17], the knee extensor mechanism was included by modeling the patellofemoral joint as one dof, where the patella moved in a constrained path about the distal femur subject to vastii and patellar tendon forces (see Fig. 1). To achieve this constrained path, the patella translated along the y-axis of the femur with translation along the x-axis and rotation about the z-axis prescribed as functions of this degree of freedom. These translations were defined as the location of the patella origin with respect to the femur origin, expressed in the femur coordinate system. With the knee in full extension, both coordinate systems were aligned with the patella initially resting in the trochlear grove [17]. There was no contact model between the patella and femur for two reasons: computational efficiency and the unavailability of high-resolution patella geometry to correspond with the open-source femur geometry [18]. Although, other sources of MRI data for a patella do exist (e.g., [13]), using bones from two different subjects for contact loads could be problematic as the trochlear groove of the femur may not necessarily match with the patellar geometry. This is important since the trochlear groove geometry has been shown to have a significant effect on patellofemoral mechanics [28].

C. Tibiofemoral Contact

Contact was modeled between the femur and tibia. The femoral articular geometry of a 77.5-kg female from an open-source finite element knee model [18] was placed on the distal end of the OpenSim bone using a least-squares fit between the surfaces in Geomagic Studio (version SR10, Parametric Technology Corp., Needham, MA, USA). For computational efficiency, the tibial plateaus were modeled as two planes with the slopes based on geometric descriptions of 23 cadaver knees [29]. The lateral plateau sloped 7° posteriorly and 2° laterally while the medial plateau sloped 2° posteriorly and medially [30], [31]. The tibial plateaus were positioned so the bones were minimally touching when knee was fully extended. Contact forces with no friction were calculated according to a linear elastic foundation model as used by [30]–[36] and implemented in OpenSim [37]. OpenSim defines the "cartilage stiffness" parameter of the elastic foundation model as the compressive modulus of the cartilage with units of stress/strain prescaled by the cartilage thickness, which results in a "cartilage stiffness" parameter with units of (stress/strain)/depth [38]. According to physiological data in the literature, cartilage stiffness ranges from 20 GN/m in the knee to 100 GN/m in the ankle joint [39]. A cartilage stiffness of 100 GN/m was used in the model to produce conservative estimates of cartilage contact loads. It is important to note the current implementation of the contact model in OpenSim does not allow the user to access how much deformation occurs in the compliant elastic foundation. Hence, force-displacement data of the model could not be obtained. Instead, the cartilage model was
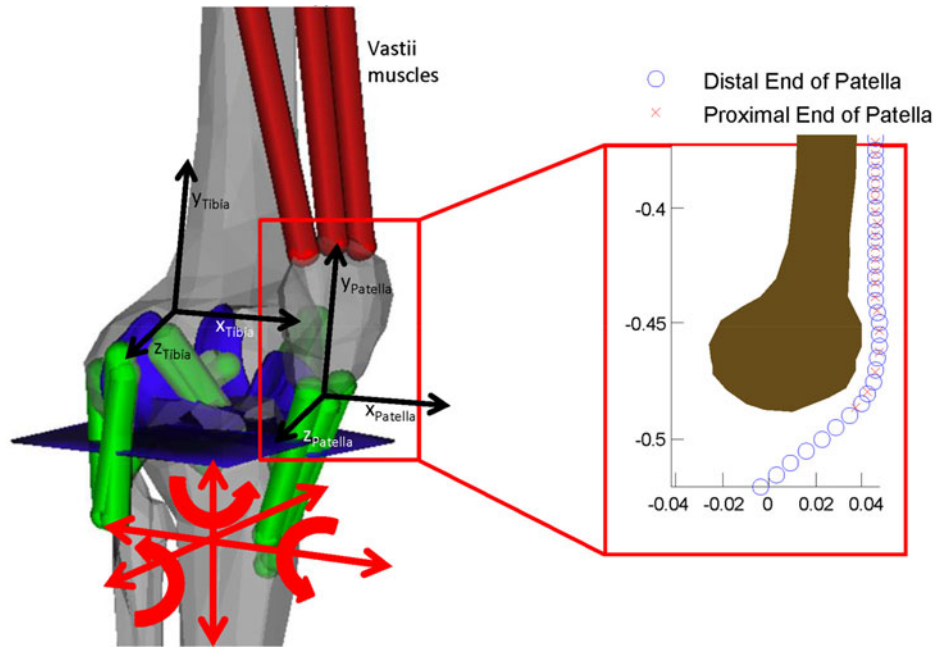
Fig. 1. Discrete element knee model created in OpenSim [21]. The tibiofemoral joint was modeled with 6 dof. The patellofemoral joint was represented with one dof where anterior–posterior translation and sagittal plane rotation were prescribed functions of superior–inferior position.

validated by comparing the cartilage contact forces of the model to experimentally measured values (as described in Section II-E. Validation of passive behavior).

D. Ligaments

Eighteen ligament bundles were included in the model (see Fig. 2): anterior cruciate ligament (ACL, 2), posterior cruciate ligament (PCL, 2), medial collateral ligament (MCL, 5), lateral collateral ligament (LCL, 1), poplitofibular ligament (PFL, 1), posterior capsule (4), and patellar tendon (3). The numbers in parenthesis represent the number of bundle fibers for each ligament. To approximate the path from origin to insertion, ligament geometries were represented as line segments [20], [40]. The origin and insertions of the ACL and PCL bundles were placed using anatomical landmarks [41]–[45] as well as the PFL and LCL [46], [47]. The MCL bundles were positioned using data by Shelburne et al., [19] with wrapping about the femur accounted for by placing spheres around the femoral epicondyles that the ligaments could not pass through (i.e., wrapping surfaces in OpenSim). The posterior capsule bundles were located according to anatomical landmarks on the posterior portion of the distal femoral epicondyles and tibial plateaus [48]. The patellar tendon was positioned according to [17]. The ligaments were modeled as nonlinear elastic springs with no damping where the force-strain relationship was defined as a quadratic toe region and subsequent linear portion after 3% strain [19], [35], [36], [49], [50]. The ligament properties, slack length and stiffness, were initially adapted from the literature [9] and minimally tuned manually to match the passive behavior of the model to that seen experimentally in the literature. The final properties are displayed in the supplemental information.

E. Validation of passive behavior

To validate the model, its passive behavior was compared to cadaveric literature as suggested by Hicks et al., and Anderson et al., [51], [52]. The literature studies [53]–[64] were chosen because the cadaveric specimen preparation was consistent across studies: transection of the limb at mid-femur and mid-tibia. Therefore, the whole femur and tibia bones were not included in the testing results and knee extensor mechanism kept intact. To compare the model simulation results with those of the cadaveric studies, only the quadriceps muscles were modeled (i.e., no hamstrings or other muscles) and gravitational effects were ignored. The vastii muscles were needed to keep the extensor mechanism intact, similar to the experimental studies.

First, the model was passively flexed up to 90° while the other five dof were left unconstrained (including varus–valgus alignment) and hence governed by ligament and contact loads. This was accomplished in OpenSim by specifying knee flexion angle as a prescribed function of time in the model file and performing a forward dynamic simulation. The five unconstrained dof were compared with [53]. The tibiofemoral contact forces during this passive motion were compared to those measured during the swing phase of gait using instrumented knee implants [14]. The swing phase of gait was used since contact force data during a slow, passive motion was not available in the literature. The swing phase of gait guarantees comparable flexion-extension knee angles to those used in [53] and no load bearing. Next, an anterior and posterior force of 100 N was applied to the tibia in order to measure the anterior–posterior translation [54]–[59]. This was accomplished in OpenSim by applying a prescribed force at the tibia origin with the knee angle fixed at 0°, 15°, 30°, 45°, 60°, 75°, and 90° of flexion. Then, an axial rotation torque of 5 N·m was applied to the tibia with the resulting rotation
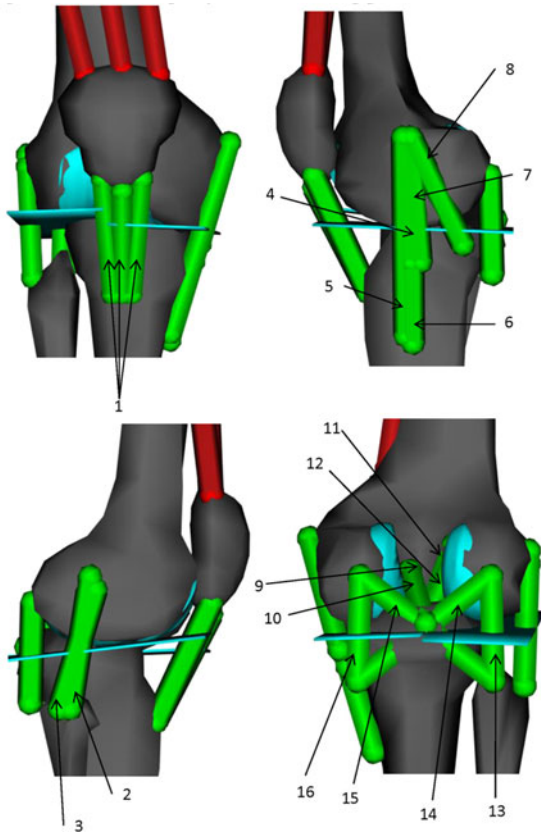
Fig. 2.   Eighteen ligament bundles were included in the model. 1: 3 bundles of the patellar tendon (PT), 2: lateral collateral (LCL), 3: popliteofibular (PFL), 4: anterior bundle of deep medial collateral (aCM), 5: anterior bundle of superficial medial collateral (aMCL), 6: central bundle of superficial medial collateral (iMCL), 7: posterior bundle of deep medial collateral (pMCL), 8: posterior bundle of superficial medial collateral (pCM), 9: anterolateral bundle of posterior cruciate (aPCL), 10: posteromedial bundle of posterior cruciate (pPCL), 11: anteromedial bundle of anterior cruciate (aACL), 12: posterolateral bundle of anterior cruciate (pACL), 13: lateral bundle of posterior capsule (CAPl), 14: oblique popliteal bundle of posterior capsule (CAPo), 15: arcuate popliteal bundle of posterior capsule (CAPa), 16: medial bundle of posterior capsule (CAPm)

measured [56]–[64]. Finally, an abduction and adduction torque of 10 N·m was applied to the tibia with the resulting rotation measured and compared with [55]–[64]. Although the model's intended use is for gait simulations, where the knee typically reaches a maximum angle of 60° [65], the passive behavior was tested up to 90° of flexion. This was done to better understand the bounds of the model.

In addition to the global passive behavior, ligament function was also compared to the literature. To validate the physiological function of the ligaments, strain in the ligaments was calculated throughout the simulations since other studies have proposed a physiological limit of 10% ligament strain [66]. The bounds and stability of the model were also investigated and is presented in the supplemental Information.

III. RESULTS

The tibia adducted 3° and internally rotated 15° as the knee flexed up to 100°, while the most posterior, tibial attachment of

the ACL translated posteriorly by 28 mm, superiorly by 2.5 mm, and medially by 6 mm (see Fig. 3). Maximum deviation of the model from the literature occurred at the most flexed angle with deviations of 2° adduction, 7° internal rotation, 1-mm posterior translation, 12-mm inferior translation, and 4-mm lateral translation. The maximum strain achieved by any ligament during the passive flexion motion was 12%, which occurred in the arcuate popliteal bundle of the posterior capsule at full extension.

The maximum tibiofemoral contact forces were seen at the most extended and flexed positions. At an extended position of 5° of flexion, the medial and lateral compartments experienced loads of 0.6 N/BW, the same as that seen during the swing phase of gait [14]. At a more flexed position of 60°, the medial compartment was loaded with 0.2 N/BW, compared to the literature of 0.22 N/BW [14], while the lateral compartment experienced 0.1 N/BW, versus the literature value of 0.22 N/BW [14]. BW denotes body weight in units of Newtons.

When 100 N of anterior force was applied, the anterior bundle of the anterior cruciate ligament (aACL) experienced the highest strain (10%) among the ligaments at lower flexion angles (see Fig. 4). At the lowest angle, full extension, the tibia translated by 2.5 mm, compare to the literature range of 1.5–6.5 mm [54]–[59]. As flexion angle increased, the ligamentous restraint to anterior translation shifted from the aACL to the anterior bundle of the medial collateral (aMCL), which displayed the highest strain of 10%. At 45° of flexion, the maximum amount of anterior translation, 4.5 mm (compared to the literature range of 3–8 mm [54]–[59]) was achieved. The model deviated the most from the literature at 90° of flexion with a translation of 0.5 mm, compared to 2–7 mm [54]–[59] in the literature, where the aMCL achieved the highest strain of 10%.

When the opposite force, 100 N of posterior load, was applied the MCL was the main restraint and showed a maximum strain of 7% at lower flexion angles (see Fig. 4). At full knee extension, the tibia translated 2.5 mm posteriorly, compared to the literature range of 1.5–7 mm [54]–[59]. As knee flexion angle increased, the PFL (8% strain) and anterior bundle of the posterior cruciate ligament (aPCL) (8% strain) increased their role in the posterior translation restraint. The maximum translation achieved was at 30° of flexion, with 7.5 mm compared to the literature range of 3.5–9 mm [54]–[59]. At 90° of flexion, the model showed the largest deviation from the literature with 1 mm of translation, versus the literature range of 2.5–6 mm.

Application of a 5 N·m internal rotation torque was restrained mainly by the posterior bundle of the medial collateral (pMCL), which displayed strains of 6–10% across all flexion angles (see Fig. 5). The minimum rotation resulting from the applied torque was seen at full extension with a result of 6°, compared to the literature range of 6–15° [56]–[64]. At 60° of flexion, the maximum rotation of 21° occurred, compared to the literature range of 6–22° [56]–[64].

An external rotation torque of 5 N·m resulted in stretching the MCL, which achieved 6–10% strain (see Fig. 5), across all flexion angles tested. The minimum rotation achieved was 9° of external rotation, compared to the literature range of 5°–15° [56]–[64], when the knee was fully extended. The maximum deviation from the literature occurred when the model
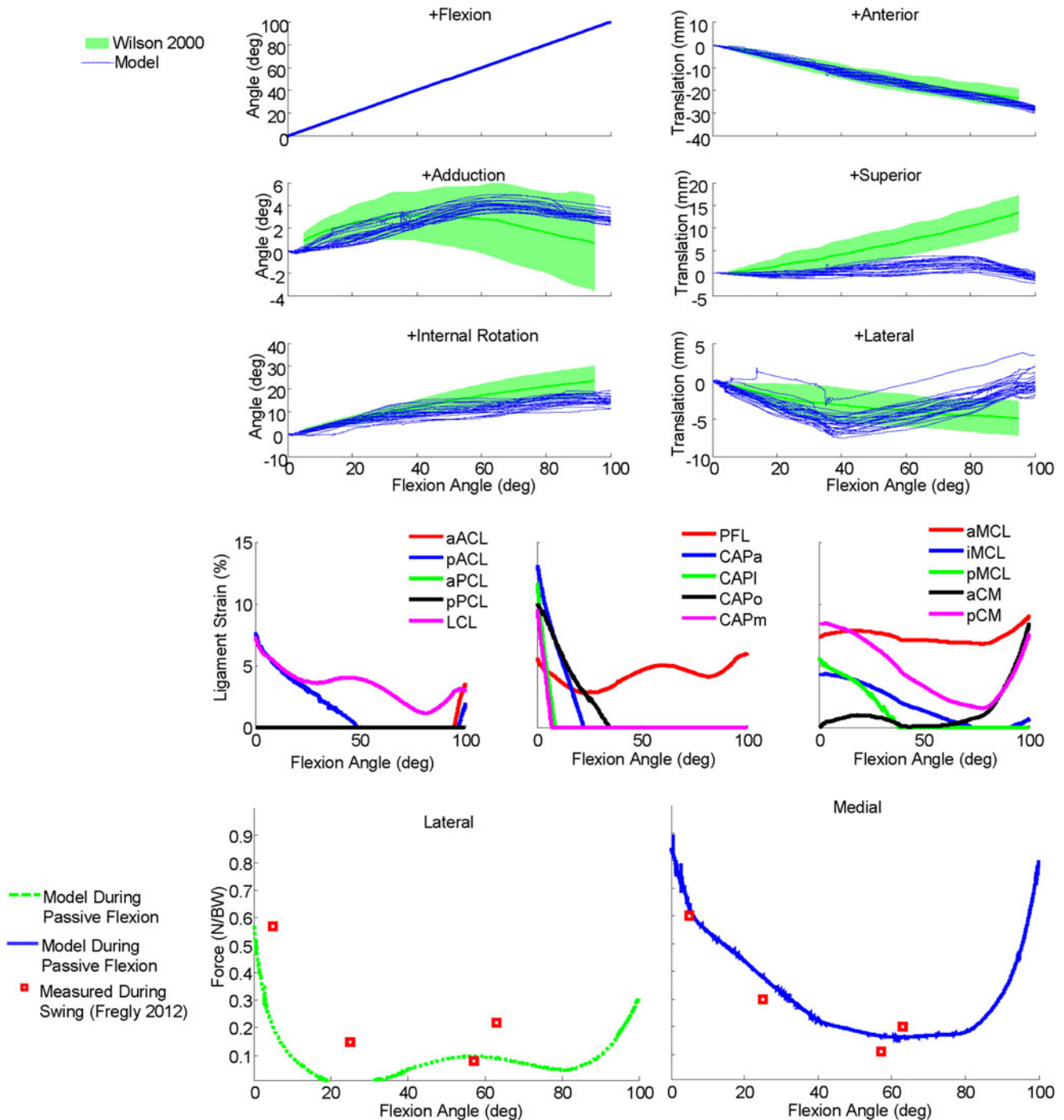
Fig. 3.   (top) Passive motion of the tibiofemoral joint compared to cadaveric data [53]. (middle) A maximum strain of 12% occurred in the CAPa ligament. (bottom) Tibiofemoral contact loads during the passive motion were 0.6 N/BW in the medial compartment and 0.8 N/BW in the lateral compartment, the same as those measured during the swing phase of gait [14].

externally rotated 24°, versus the literature range of 10–22°, at 75° of knee flexion [56]–[64].

An adduction torque of 10 N·m caused the model to adduct by 0.5–5°, compared to the literature range of 1°–13°, across all degrees of knee flexion (see Fig. 6). This adduction torque caused the posterior bundle of the anterior cruciate ligament (pACL) to have the largest strain, 7%, at full extension. As knee flexion angle increased, the adduction moment restraint

shifted to the PFL, LCL, and MCL bundles with strains of 6–10%.

The application of 10N·m of abduction torque resulted in straining the pACL to 9% at full extension (see Fig. 6). The lowest amount of abduction rotation, 1° versus the literature range of 2–8° [55]–[64], was also seen a full knee extension. As knee flexion increased, the MCL restraint also increased by reaching strains of 6–10%. This also resulted in increasing
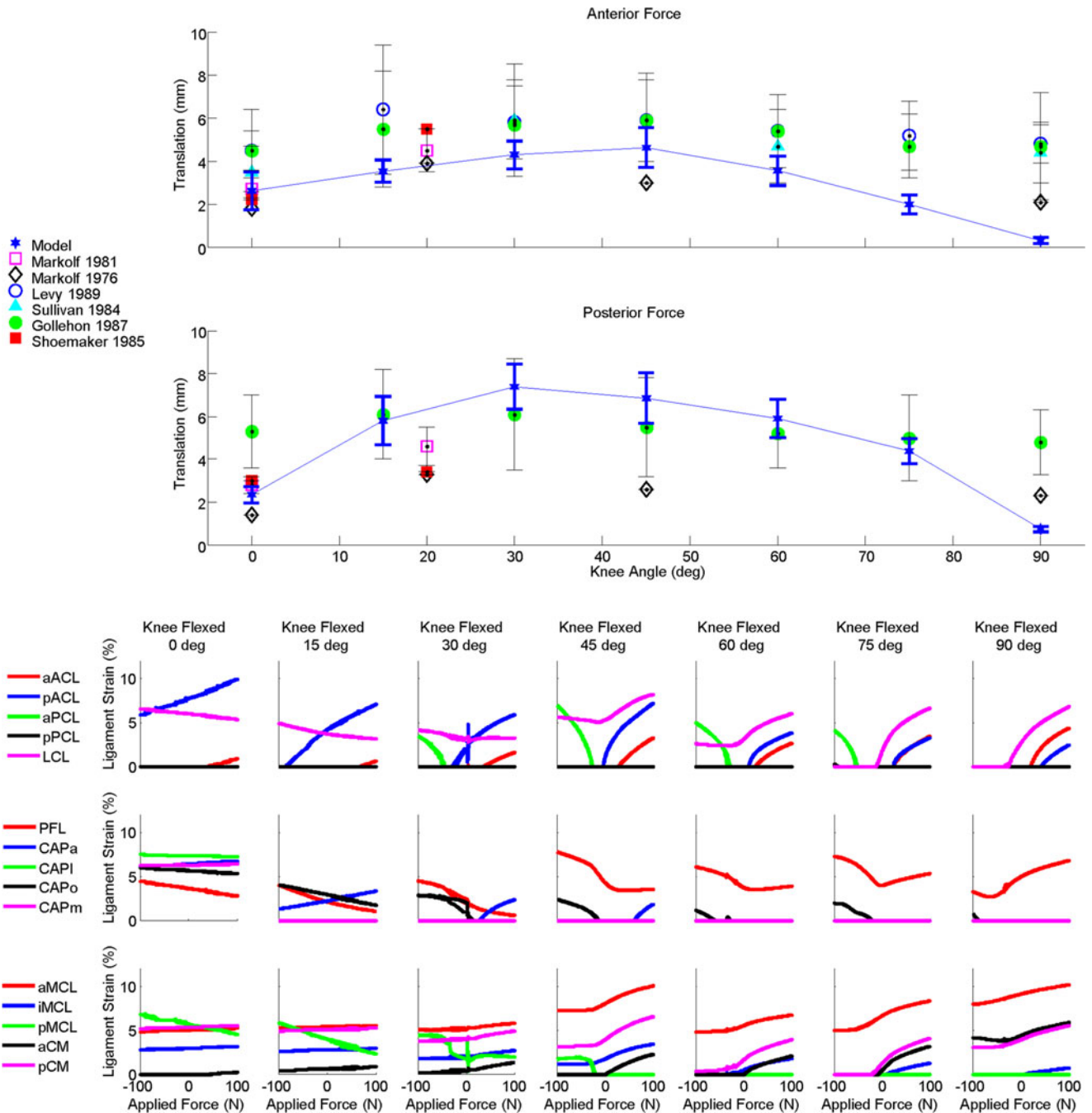
Fig. 4. (top) With 100 N of applied force, the model translated 0.5–4.5 mm anteriorly, compared to the literature range of 2–9 mm [54]–[59]. Posteriorly, the model translated 0.5–7 mm, versus the literature range of 1.5–8.5 mm. (bottom) When an anterior force was applied, the aACL achieved the largest strain at lower flexion angles. As flexion angle increased, the ligamentous restraint to anterior translation shifted from the aACL to the aMCL, When the opposite force, 100 N of posterior load, was applied the MCL was the main restraint at lower flexion angles. As knee flexion angle increased, the PFL and aPCL increased their role in the posterior translation restraint.

abduction angles of 2°–6°, compared to the literature range of 2°–14° [55]–[64].

IV. DISCUSSION

This paper presents a validated, open-source, discrete element model of the knee. Discrete element models offer a balance between simplified kinematic joints and finite element models by providing soft tissue loads at a low computational cost. Before this study, there was not an open-source, discrete element knee model available in the literature. One reason may be due to the complexity and time it takes to create a well-crafted model. The model presented in this paper is physiologically reasonable as demonstrated by comparing its passive behavior, ligament properties, ligament function, and contact forces with the literature. This model is the first open-source
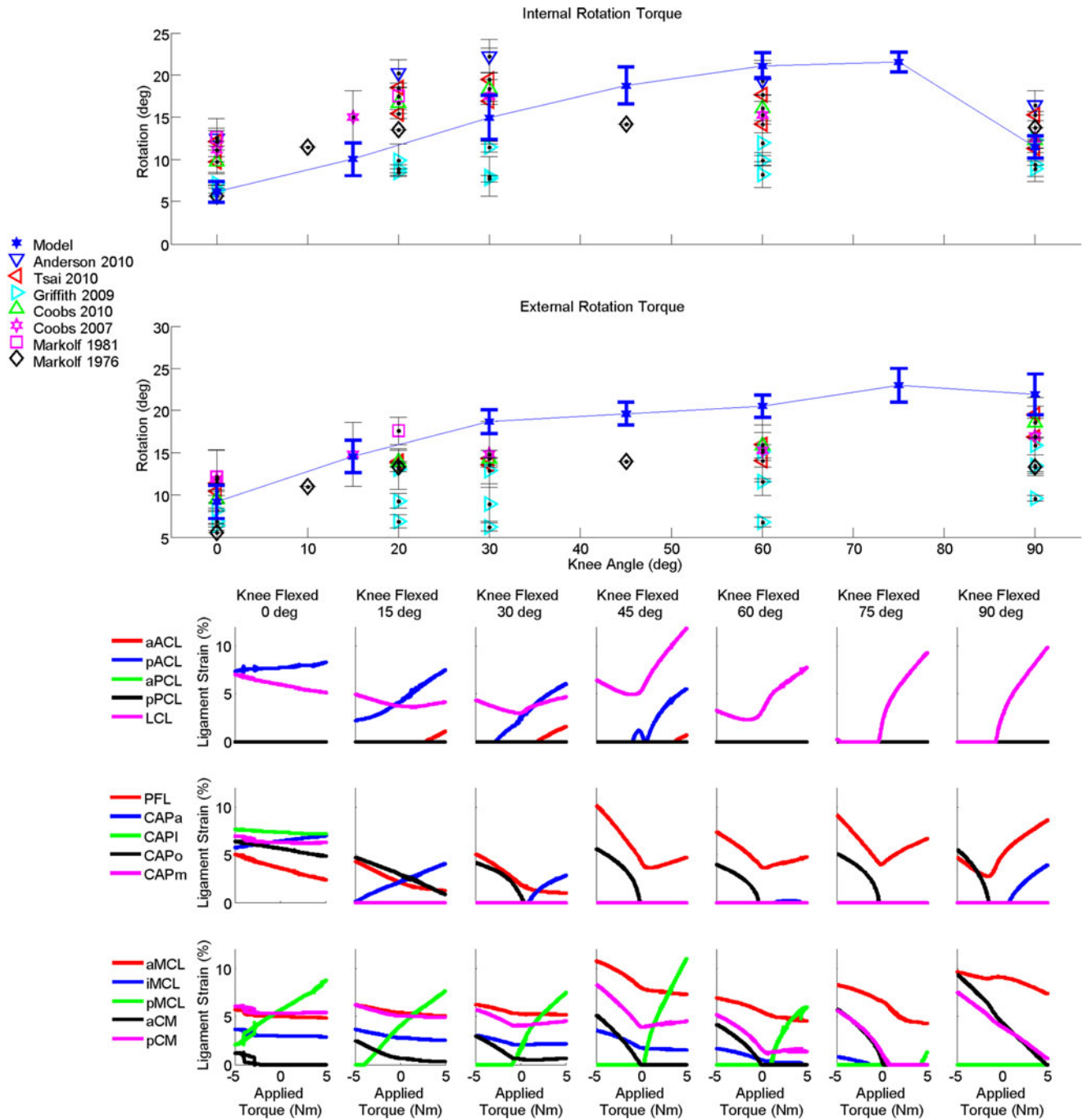
Fig 5. (top) When 5 N·m of axial torque was applied, the model internally rotated by 6–20°, compared to the literature range of 5–22° [56]–[64]. The model rotated 10 – 21 deg externally, versus the literature range of 0 – 21 deg. (bottom) Application of an axial rotation torque was restrained mainly by the MCL bundles, which showed a maximum torque of 11% at 45 deg of knee flexion.

knee model of this type, making modeling a more accessible tool for biomechanists. This model can be freely downloaded from https://simtk.org/home/kneemodel/ as an OpenSim model, .osim file, and opened in the free software, OpenSim https://simtk.org/home/opensim.

The anterior–posterior motion of the knee showed reasonable behavior. As the knee was passively flexed, the tibial attachment of the ACL translated posteriorly by 28 mm with a maximum deviation of 1 mm from the literature at the most flexed angle

(see Fig. 3). When an anterior force was applied, the tibia translated anteriorly 0.5–4.5 mm (compared to the literature range of 2–9 mm) with the main restraint due to the aACL and aMCL (see Fig. 4). These restraints agree with other studies that have found the ACL to be the primary restraint to anterior translation and the MCL as a secondary restraint [43], [67]. In fact, the sensitivity analysis (supplemental info) showed the anterior translations to be affected mostly by the slack lengths set for the ACL and MCL (Fig. S1). However, further loosening of these
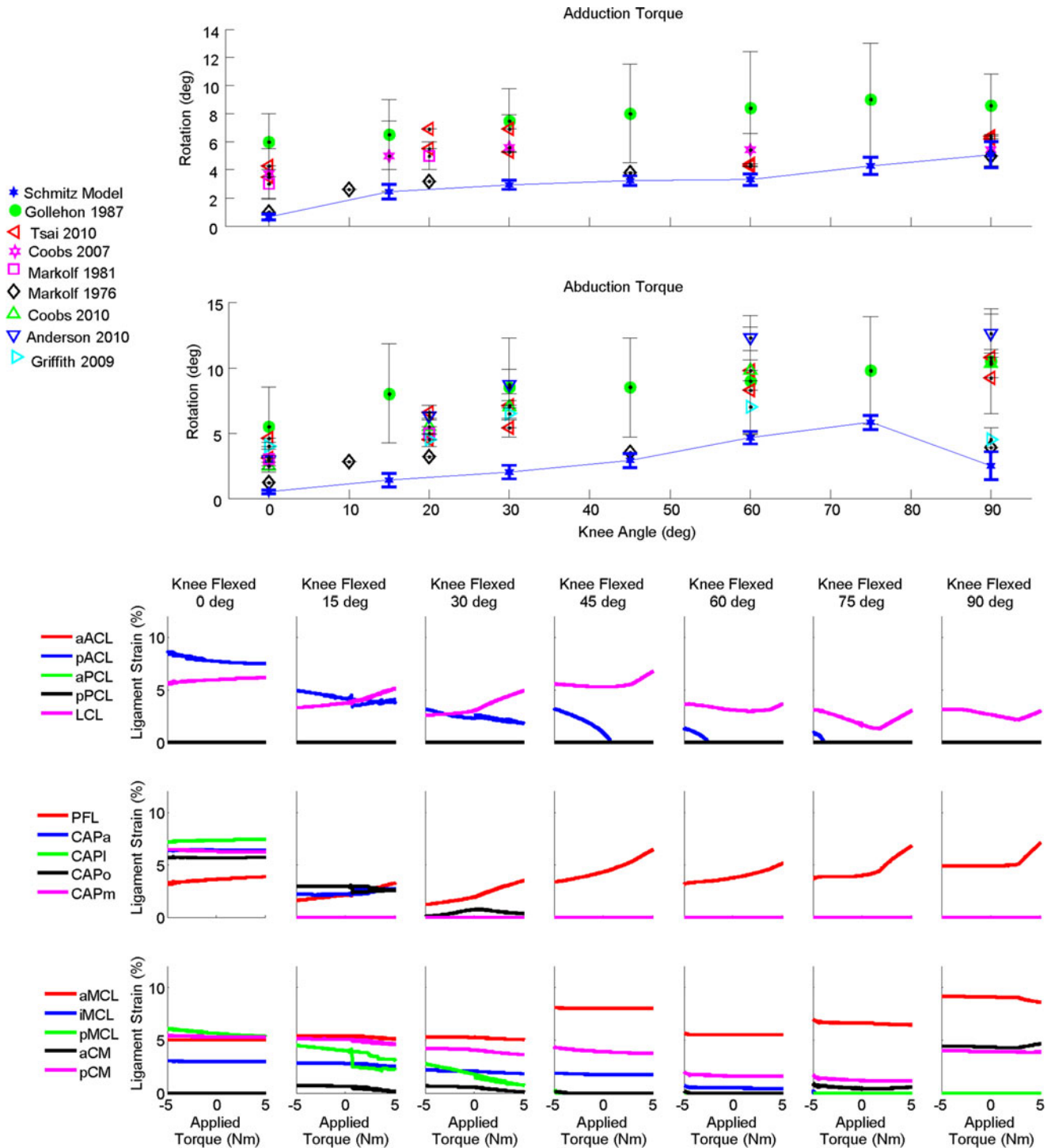
Fig. 6. (top) A 10 N·m ab-adduction torque caused the model to ab-adduct by 0.5–5°, versus the literature range of 1–14° [55]–[64]. (bottom) This adduction torque caused the pACL to have the largest strain. As knee flexion angle increased, the adduction moment restraint shifted to the PFL, LCL, and MCL bundles. The application of an abduction torque resulted in straining the pACL at full extension and the MCL bundles at more flexed angles.

parameters to increase the model's translation, and hence agree better with the literature, caused intercondylar liftoff during the passive flexion motion. Besides ligament properties, the tibial plateau geometry is another factor that may influence the anterior behavior of the model since increased tibial slope may also increase anterior translation [68]. When a posterior force was applied, the tibia translated 0.5–7 mm (as opposed to the literature range of 1.5–8 mm) and was mainly restrained by the MCL, PFL, and PCL. This qualitatively agrees with studies on ligament function that have shown the PCL to be the primary posterior translation restraint [43], [67]. The large contributions from the MCL and PFL are likely due to where these ligaments

were placed in the model. However, the MRI data used to obtain the open-source bones did not provide enough information to extract ligament placement sites [18].

The knee showed reasonable axial rotation behavior. As the model was passively flexed, the tibia exhibited the screw-home mechanism by internally rotating 15° which deviates from the literature by 7° (see Fig. 3). When 5 N·m of axial torque was applied, the model internally rotated by 6–20° (compared to the literature range of 5–22°) and rotated 10–21° externally (versus the literature range of 0–21°) (see Fig. 5). The axial rotation was restrained mainly by the MCL bundles, which agrees with literature on ligament function [55]–[71]. The axial rotation behavior of this model is novel since few, if any, models in current literature either include this degree of freedom or have validated it.

The model was stiff in the frontal plane. The tibia adducted 3° during passive flexion, which deviated by 2° from the literature (see Fig. 3). An ab-adduction torque caused the model to ab-adduct by 0.5–5° (as opposed to the literature range of 1–14°), across all degrees of knee flexion (see Fig. 6). The ab-adduction moment was restrained by the PFL, LCL, and MCL bundles, which is also consistent with the literature on ligament function [55]–[71]. Therefore, the low ab-adduction angles seen are likely a result of the cartilage model used. More work is needed to better ascertain the meaning of cartilage stiffness in the OpenSim contact model and how this parameter affects the model behavior.

As the tibia was passively flexed, the most posterior, tibial attachment of the ACL translated superiorly by 2.5 mm with a maximum deviation from the literature of 12 mm at the most flexed angle (see Fig. 3). The superior–inferior motion is most likely a function of the roll-back mechanism of the femur. Therefore, this is probably governed by the geometry of the femur and tibia. More work is needed to assess the sensitivity of the superior–inferior motion to model parameters, e.g., size of femoral condyles. Although the effect of tibial plateau angle and femur geometry on anterior–posterior motion has been well studied in the literature (e.g., [68]), the effect of contact geometry on superior-inferior motion is not well documented. Since our model with planar plateaus predicted more superior–inferior translation than cadaveric studies, we hypothesize adding physiological tibial plateaus with a more conforming geometry would loosen the ligaments and decrease the overall stiffness of the model (e.g., increase anterior-posterior translation with application of 100 N). Although, more work is needed to explicitly elucidate the sensitivity of ligament function and overall model behavior to tibial geometry parameters (e.g., slopes, physiological tibia from MRI, etc.). Furthermore, contact does not occur between the two bone surfaces as the menisci are interposed between the surfaces. In fact, deformation of the menisci varies between 1-2 mm [72]. This deformation is comparable with the variation in surface level of an anatomical tibia. Using a more precise surface without considering the proper deformation of the cartilage would be speculative.

The ligament properties in the model were compared to the literature. Other modeling studies have proposed a physiological limit of 10% ligament strain during passive motion [66]. The maximum ligament strain achieved during the passive flexion motion of the knee model of this study was 12% (see Fig. 3) and 10% during the stiffness simulations (see Figs. 4–6), which is close agreement to the limit proposed by Blankevoort et al. [66], adding to the validation of the ligament slack lengths. In vivo measurements of ACL strain during active flexion-extension have been shown to vary from 3% at more extended angles to -2% at 60° of flexion [73]. These *in vivo* values are lower than the 7% strain experienced by the ACL in our model. One explanation for the increased strain could be the planar geometries used for the tibial plateaus. Anatomically, the tibial plateaus are more conforming to the femoral condyles, which may cause decreased superior–inferior translation and, hence, decreased ACL stretch. A thorough comparison of the stiffness and slack length properties of the ligaments with those of tensile testing and other discrete element models can be found in the supplemental information.

The maximum tibiofemoral contact forces were seen at the most extended and flexed positions. At an extended position of 5° of flexion, the medial and lateral compartments experienced loads of 0.6 N/BW, the same as that seen during the swing phase of gait [14]. At a more flexed position of 60°, the medial compartment was loaded with 0.2 N/BW while the lateral compartment experienced 0.1 N/BW, versus the literature value of 0.22 N/BW for both compartments [14]. The largest deviation of the model from the literature was an underestimation of the model by 0.12 N/BW, which occurred in the lateral compartment. This discrepancy could be due to inertial effects during the swing phase of gait that were not present in the model simulation.

There are some study design factors and limitations of the model that should be noted. First, there are some deviations between the model behavior and literature: low translations and rotations seen at full extension and flexion. However, this could be due to a limitation of the field in that the model components come from different sources: generic bony geometry based on cadavers [22], muscle and ligament attachments established using the anatomical landmarks of these bones, articular geometry of the femur from MRI data of a single specimen [18], tibial plateaus based on cadaveric data [29], and ligament properties adapted from other models and tensile testing of cadaver tissue (see Table 1 of the supplemental information). A second limitation of the model is the simplified patellofemoral joint and tibial geometry. This was done to increase computational speed. Using a 64-bit computer with 16.0 GB of random access memory and an Intel Core i5-4590 CPU at 3.30 GHz, the model takes 15 min to run one of the stiffness simulations (e.g., apply 100 N of anterior force, then 100 N of posterior force, at a fixed flexion angle), with the resulting files 79 MB in size. In fact, including MRI geometry for more than one bone in the contact calculations, e.g., physiological femur and tibia from MRI as .stl files, caused OpenSim to fail. As OpenSim evolves in computational speed and efficiency, future work can add physiological tibia geometry and a 6 dof patellofemoral joint. Third, the model was validated for static conditions. It is important to establish the validity of the model under passive, static conditions before adding more complex structures like muscles. Fourth, menisci were not included in the model as they mainly act as shock absorbers

and load transmitters, as opposed to translational and rotational restraints [74], [75]. Finally, although the model was not explicitly tested in various sizes to show its scalability, this model can be scaled to multiple patient sizes but may require tuning (e.g., method proposed by Shelburne [76]) to ensure reasonable passive behavior for each size.

A particular study design factor that warrants further discussion is the simplification of the tibial plateaus as planes. Other models have used physiological tibial plateaus from MRI (e.g., [77]). A model using planes instead of a physiological conforming tibial geometry likely underestimates the cartilage contact area, which would lead to an overestimation of contact loads. However, more work is needed to better ascertain the effect of tibia geometry on arthrokinematics. The tibiofemoral contact was also modeled as frictionless. If the friction between the two surfaces cannot be neglected, we could assume that an increase in contact force between the femur and the tibial plateau is generated by the elasto-hydronamic (EHD) effect of the fluid viscosity. This additional force component is strictly due to the movement between the two surfaces and the geometry change (conformity) between the two surfaces. The EHD effect could be added to the effect of the inertial forces due to the movement. EHD forces can be determined via Reynold's Equations commonly used in the tribology field in

$$\frac{\partial}{\partial x}\left(h^3\frac{\partial P}{\partial x}\right) + \frac{\partial}{\partial z}\left(h^3\frac{\partial P}{\partial z}\right) = 6\eta\frac{\partial\left\{(U_f - U_t)\,h\right\}}{\partial x}$$

$$+12\eta\frac{\partial h}{\partial t} + 6\eta\frac{\partial\left\{(W_f - W_t)\,h\right\}}{\partial x}. \tag{1}$$

In the above equation, P is the pressure of the fluid, x is the curvilinear coordinate tangent to the tibial plateau, z is orthogonal to x pointing medio-laterally, h is the fluid film thickness, η is the viscosity of the fluid, U_f is the tangential velocity of the femur along x, and U_t is the velocity of the tibial plateau tangential to the ground. And, using the same subscripts W represents the velocity component of femur and tibia orthogonal to x pointing upward (y). It is immediate to see that if η is negligible, the pressure gradient generated by the fluid will be zero. The terms depending on W and U at the second member are called wedge actions and can generate force combining two different mechanism. Using the term $\frac{\partial\{(U_f - U_t)h\}}{\partial x}$ as an example, we can have that:

1) $\frac{\partial\{h\}}{\partial x} = 0$ but $\frac{\partial\{(U_f - U_t)\}}{\partial x} \neq 0$: This happens when there is no wedge between surfaces but the two surfaces are stretchy and generate a peristaltic effect.
2) $\frac{\partial\{h\}}{\partial x} \neq 0$ but $\frac{\partial\{(U_f - U_t)\}}{\partial x} = 0$: This happens when the two surfaces are transversally stiff but they form a wedge

The term $12\eta\frac{\partial h}{\partial t}$ represents a squeezing effect between the two surfaces. It should be noted that classical Reynold's equations are subject to numerous assumptions such as:
1) negligible inertia of the fluid;
2) negligible pressure gradient in the direction of the film thickness (y);
3) Newtonian fluid;
4) constant value of viscosity;
5) no slip at solid boundary;

6) neglecting angle of inclination for curved surface;
7) incompressible fluid flow; and
8) relative tangential velocity only in caudal-frontal direction.

Another simplification used in the model is a 1 dof patellofemoral joint, versus a fully 6 dof patella. Other models have used a fully 6 dof patella with a 6 dof tibia [77]. Patellofemoral contact is needed in a cosimulation framework, where patellofemoral contact or geometry is the focus of study. This limits the use of the current model to tibiofemoral contact and ligaments. We hypothesize the constrained patellofemoral path would have little effect on tibiofemoral measures since nonsagittal movement is negligible compared to the sagittal plane motion [78]. Although, more work is needed to directly test the effect of patellofemoral joint model on model outcomes as little data exists in the literature.

One constraint of the field that poses a challenge to model reproducibility and validation is that the model components come from different sources: generic bony geometry based on cadavers [22], muscle and ligament attachments established using the anatomical landmarks of these bones, articular geometry of the femur from MRI data of a single specimen [18], tibial plateaus based on cadaveric data [29], and ligament properties adapted from other models and tensile testing of cadaver tissue (see Table 1 of the supplemental information). Currently, there is no study that contains all of these components for a single or group of healthy subjects. Another challenge in the modeling field is sharing. Many models are developed in costly software packages and not made publicly available. This hinders the forward progression of the modeling field, both in research and the ability to educate students to become future modelers. This is the first study, so far, to share a validated discrete element knee model with ligaments and contact that can be used as a direct plugin with the freeware platform OpenSim.

This model has many applications. First, the model could be used to probe the influence of ligament placement and contact geometry on passive knee mechanics. This is the next step to perform before the model can be used in dynamic simulations. After this step, the model could be incorporated into a serial simulation to predict soft tissue loading during movement (e.g., [33]) or in a cosimulation framework, where muscle forces and soft tissue mechanics are simultaneously predicted. The model could be used to create a surrogate model of knee behavior, the uses of which have shown great promise in making cosimulation methods run quickly [79]. For example, how does ACL placement affect the rotational stiffness? This might have implications for ACL reconstructive surgery. However, before the model could be used to predict soft tissues loads, the soft tissue loads (e.g., cartilage contact loads) predicted during gait should be validated as well. This could be done using the freely available Grand Challenge Data that consist of instrumented motion analysis and cartilage loads from an instrumented knee implant (https://simtk.org/home/kneeloads, [14]).

V. CONCLUSION

In summary, a discrete element knee model has been presented. Through a comparison with the literature, the model

has shown physiologically reasonable passive motion, stiffness, ligament properties, ligament function, and contact forces. A novel element of the model is that it is open source and freely available for download at https://simtk.org/home/kneemodel/. This enables more researchers to add to the refinement of the model as well as providing modeling as an accessible tool to a wider audience.

ACKNOWLEDGMENT

There are no funding sources or conflicts of interest to disclose.

REFERENCES

[1] M. A. Dunkin, "Handout on health: Sports injuries," 2009.

[2] S. A. Oliveria *et al.*, "Incidence of symptomatic hand, hip, and knee osteoarthritis among patients in a health maintenance organization," *Arth. Rheu.*, vol. 38, no. 8, pp. 1134–1141, 2005.

[3] T. Asano *et al.*, "The functional flexion-extension axis of the knee corresponds to the surgical epicondylar axis: In vivo analysis using a biplanar image-matching technique," *J. Arthro.*, vol. 20, pp. 1060–1067, 2005.

[4] J. A. Reinbolt *et al.*, "Determination of patient-specific multi-joint kinematic models through two-level optimization," *J. Biomech.*, vol. 38, pp. 621–626, 2005.

[5] Y. Y. Dhaher *et al.*, "The effect of connective tissue material uncertainties on knee joint mechanics under isolated loading conditions," *J. Biomech.*, vol. 43, no. 16, pp. 3118–3125, 2010.

[6] M. M. van der Krogt *et al.*, "How robust is human gait to muscle weakness?" *Gait Posture*, vol. 36, no. 1, pp. 113–119, 2012.

[7] K. B. Shelburne *et al.*, "Effect of muscle compensation on knee instability during acl-deficient gait," *Med. Sci. Sports Exerc.*, vol. 37, no. 4, pp. 642–648, 2005.

[8] Y. Dhaher and L. Kahn, "The effect of vastus medialis forces on patellofemoral contact: A model-based study," *J. Biomech. Eng.*, vol. 124, pp. 758–767, 2002.

[9] A. Schmitz, "The importance of including knee joint laxity in dynamic musculoskeletal simulations of movement," Ph.D. dissertation, Biomed. Eng. Univ. Wisconsin-Madison, Madison, WI, USA, 2012.

[10] J. P. Halloran *et al.*, "Adaptive surrogate modeling for efficient coupling of musculoskeletal control and tissue deformation models," *J. Biomech. Eng.*, vol. 131, no. 1, pp. 011014–011017, 2009.

[11] Y. C. Lin *et al.*, "Simultaneous prediction of muscle and contact forces in the knee during gait," *J. Biomech.*, vol. 43, no. 5, pp. 945–952, 2010.

[12] D. Thelen *et al.*, "Simultaneous prediction of muscle, ligament and tibiofemoral contact forces via optimally tracking subject-specific gait dynamics," presented at the Summer Bioeng. Conf., Sunriver, OR, USA, 2013.

[13] T. M. Guess *et al.*, "A multibody knee model with discrete cartilage prediction of tibio-femoral contact mechanics," *Comput. Meth. Biomech. Biomed. Eng*, vol. 16, no. 3, pp. 256–270, 2013.

[14] B. J. Fregly *et al.*, "Grand challenge competition to predict in vivo knee loads," *J. Orthop. Res.*, vol. 30, no. 4, pp. 503–513, 2012.

[15] A. L. Kinney *et al.*, "Update on grand challenge competition to predict in vivo knee loads," *J. Biomech. Eng.*, vol. 135, no. 2, p. 021012, 2013.

[16] D. G. Thelen *et al.*, "Co-simulation of neuromuscular dynamics and knee mechanics during human walking," *J. Biomech. Eng.*, vol. 136, no. 2, p. 021033, 2014.

[17] E. M. Arnold *et al.*, "A model of the lower limb for analysis of human movement," *Ann. Biomed. Eng.*, vol. 38, no. 2, pp. 269–279, 2010.

[18] S. Sibole *et al.*, "Open knee: A 3d finite element representation of the knee joint," presented at the 34th Annual Meeting of the American Society of Biomechanics, Providence, RI, USA, 2010.

[19] K. B. Shelburne *et al.*, "Contributions of muscles, ligaments, and the ground reaction force to tibiofemoral joint loading during normal gait," *J. Orthop. Res.*, vol. 24, no. 10, pp. 1983–1990, 2006.

[20] H. Xu *et al.*, "An improved opensim gait model with multiple degrees of freedom knee joint and knee ligaments," *Comp. Meth. Biomech. Biomed. Eng.*, vol. 18, no. 11, pp. 1217–1224, 2015.

[21] S. L. Delp *et al.*, "Opensim: Open-source software to create and analyze dynamic simulations of movement," *IEEE Trans. Biomed. Eng.*, vol. 54, no. 11, pp. 1940–1950, Nov. 2007.

[22] S. L. Delp *et al.*, "An interactive graphics-based model of the lower extremity to study orthopaedic surgical procedures," *IEEE Trans. Biomed. Eng.*, vol. 37, no. 8, pp. 757–767, Aug. 1990.

[23] G. T. Yamaguchi and F. E. Zajac, "A planar model of the knee joint to characterize the knee extensor mechanism," *J. Biomech.*, vol. 22, no. 1, pp. 1–10, 1989.

[24] F. C. Anderson and M. G. Pandy, "A dynamic optimization solution for vertical jumping in three dimensions," *Comput. Meth. Biomech. Biomed. Eng.*, vol. 2, no. 3, pp. 201–231, 1999.

[25] F. C. Anderson and M. G. Pandy, "Dynamic optimization of human walking," *Trans. Amer. Soc. Mech. Eng. J. Biomech. Eng.*, vol. 123, no. 5, pp. 381–390, 2001.

[26] A. Schmitz *et al.*, "Variables during swing associated with decreased impact peak and loading rate in running," *J. Biomech.*, vol. 47, pp. 32–38, 2013.

[27] A. S. Arnold *et al.*, "Do the hamstrings and adductors contribute to excessive internal rotation of the hip in persons with cerebral palsy?" *Gait Posture*, vol. 11, no. 3, pp. 181–190, 2000.

[28] C. M. Powers, "Patellar kinematics, part ii: The influence of the depth of the trochlear groove in subjects with and without patellofemoral pain," *Phys. Ther.*, vol. 80, no. 10, pp. 965–973, 2000.

[29] A. Garg and P. S. Walker, "Prediction of total knee motion using a three-dimensional computer-graphics model," *J. Biomech.*, vol. 23, no. 1, pp. 45–53, 55–58, 1990.

[30] M. G. Pandy *et al.*, "A three-dimensional musculoskeletal model of the human knee joint. Part 1: Theoretical construction," *Comput. Meth. Biomech. Biomed. Eng.*, vol. 1, no. 2, pp. 87–108, 1997.

[31] S. Kim, "A three-dimensional dynamic musculoskeletal model of the human knee joint," *thesis, Univ. Texas at Austin, Austin, TX, USA*, 1996.

[32] D. D. Anderson *et al.*, "Implementation of discrete element analysis for subject-specific, population-wide investigations of habitual contact stress exposure," *J. Appl. Biomech*, vol. 26, no. 2, p. 215, 2010.

[33] K. B. Shelburne *et al.*, "Pattern of anterior cruciate ligament force in normal walking," *J. Biomech.*, vol. 37, no. 6, pp. 797–805, 2004.

[34] D. Caruntu and M. Hefzy, "3-d anatomically based dynamic modeling of the human knee to include tibio-femoral and patello-femoral joints," *J. Biomech. Eng.*, vol. 126, pp. 44–53, 2004.

[35] L. Blankevoort and R. Huiskes, "Ligament-bone interaction in a three-dimensional model of the knee," *J. Biomech. Eng.*, vol. 113, pp. 263–269, 1991.

[36] L. Blankevoort *et al.*, "Articular contact in a three-dimensional model of the knee," *J. Biomech.*, vol. 24, no. 11, pp. 1019–1031, 1991.

[37] M. A. Sherman *et al.*, "Simbody: Multibody dynamics for biomedical research," *Procedia IUTAM*, vol. 2, pp. 241–261, 2011.

[38] O. Sim, "Trouble with contact," *Public Forum: OpenSim*, vol. 2016, p. 2013.

[39] D. Shepherd and B. Seedhom, "Thickness of human articular cartilage in joints of the lower limb," *Ann. Rheu. Dis.*, vol. 58, no. 1, pp. 27–34, 1999.

[40] H. Xu, "Development of a musculoskeletal model to determine knee contact force during walking on ballast using opensim simulation," *thesis, The Univ, Utah*, Salt Lake City, UT, USA, 2013.

[41] H. Gray, *Anatomy of the Human Body*. Lea & Febiger, 1918.

[42] A. Edwards *et al.*, "The attachments of the fiber bundles of the posterior cruciate ligament: An anatomic study," *Arthro: J. Arthro. Rel. Surg.*, vol. 23, no. 3, pp. 284–290, 2007.

[43] F. G. Girgis *et al.*, "The cruciate ligaments of the knee joint: Anatomical, functional and experimental analysis," *Clin. Orthop. Relat. Res.*, vol. 106, pp. 216–231, 1975.

[44] S. Kopf *et al.*, "A systematic review of the femoral origin and tibial insertion morphology of the ACL," *Knee Surg., Sports Traumatol, Artho.*, vol. 17, no. 3, pp. 213–219, 2009.

[45] W. M. D. Petersen and T. M. D. Zantop, "Anatomy of the anterior cruciate ligament with regard to its two bundles," *Clin. Orthop. Relat. Res.*, vol. 454, pp. 35–47, 2007.

[46] H. Davies *et al.*, "The posterolateral corner of the knee: Anatomy, biomechanics and management of injuries," *Injury*, vol. 35, no. 1, pp. 68–75, 2004.

[47] B. R. Meister *et al.*, "Anatomy and kinematics of the lateral collateral ligament of the knee," *Amer. J. Sports Med.*, vol. 28, no. 6, p. 869, 2000.

[48] E. M. Abdel-Rahman and M. Hefzy, "Three-dimensional dynamic behaviour of the human knee joint under impact loading," *Med. Eng. Phys.*, vol. 20, pp. 276–290, 1998.

[49] K. B. Shelburne *et al.*, "Effect of posterior tibial slope on knee biomechanics during functional activity," *J. Orthop. Res.*, vol. 29, no. 2, pp. 223–231, 2011.

[50] J. Wismans *et al.*, "A three-dimensional mathematical model of the knee-joint," *J. Biomech.*, vol. 13, no. 8, pp. 677–679, 681–685, 1980.

[51] J. L. Hicks *et al.*, "Is my model good enough? Best practices for verification and validation of musculoskeletal models and simulations of movement," *J. Biomech. Eng.*, vol. 137, no. 2, p. 020905, 2015.

[52] A. E. Anderson *et al.*, "Verification, validation and sensitivity studies in computational biomechanics," *Comput. Meth. Biomech. Biomed. Eng.*, vol. 10, no. 3, pp. 171–184, 2007.

[53] D. Wilson *et al.*, "The components of passive knee movement are coupled to flexion angle," *J. Biomech.*, vol. 33, no. 4, pp. 465–473, 2000.

[54] I. M. Levy *et al.*, "The effect of lateral meniscectomy on motion of the knee," *J. Bone Joint Surg. Amer.*, vol. 71, no. 3, pp. 401–406, 1989.

[55] D. L. Gollehon *et al.*, "The role of the posterolateral and cruciate ligaments in the stability of the human knee. A biomechanical study," *J. Bone Joint Surg. Amer.*, vol. 69, no. 2, pp. 233–242, 1987.

[56] S. C. Shoemaker and K. L. Markolf, "Effects of joint load on the stiffness and laxity of ligament-deficient knees. An in vitro study of the anterior cruciate and medial collateral ligaments," *J. Bone Joint Surg. Amer.*, vol. 67, no. 1, pp. 136–146, 1985.

[57] D. Sullivan *et al.*, "Medical restrains to anterior-posterior motion of the knee," *J. Bone Joint Surg. Amer.*, vol. 66, no. 6, pp. 930–936, 1984.

[58] K. L. Markolf *et al.*, "The role of joint load in knee stability," *J. Bone Joint Surg. Amer.*, vol. 63, no. 4, pp. 570–585, 1981.

[59] K. L. Markolf *et al.*, "Stiffness and laxity of the knee–the contributions of the supporting structures. A quantitative in vitro study," *J. Bone Joint Surg. Amer.*, vol. 58, no. 5, pp. 583–594, 1976.

[60] C. J. Anderson *et al.*, "Kinematic impact of anteromedial and posterolateral bundle graft fixation angles on double-bundle anterior cruciate ligament reconstructions," *Amer. J. Sports Med.*, vol. 38, no. 8, p. 1575, 2010.

[61] A. G. Tsai *et al.*, "Comparative kinematic evaluation of all-inside single-bundle and double-bundle anterior cruciate ligament reconstruction," *Amer. J. Sports Med.*, vol. 38, no. 2, pp. 263–272, 2010.

[62] C. J. Griffith *et al.*, "Medial knee injury: Part 1, static function of the individual components of the main medial knee structures," *Amer. J. Sports Med.*, vol. 37, no. 9, pp. 1762–1770, 2009.

[63] B. R. Coobs *et al.*, "An in vitro analysis of an anatomical medial knee reconstruction," *Amer. J. Sports Med.*, vol. 38, no. 2, pp. 339–347, 2010.

[64] B. R. Coobs *et al.*, "Biomechanical analysis of an isolated fibular (lateral) collateral ligament reconstruction using an autogenous semitendinosus graft," *Amer. J. Sports Med.*, vol. 35, no. 9, pp. 1521–1527, 2007.

[65] M. P. Kadaba *et al.*, "Measurement of lower extremity kinematics during level walking," *J. Orthop. Res.*, vol. 8, no. 3, pp. 383–392, 1990.

[66] L. Blankevoort *et al.*, "Recruitment of knee joint ligaments," *J. Biomech. Eng.*, vol. 113, no. 1, pp. 94–103, 1991.

[67] K. F. Bowman Jr and J. K. Sekiya, "Anatomy and biomechanics of the posterior cruciate ligament, medial and lateral sides of the knee," *Sports Med. Arthro Rev.*, vol. 18, no. 4, p. 222, 2010.

[68] J. R. Giffin *et al.*, "Effects of increasing tibial slope on the biomechanics of the knee," *Amer. J. Sports Med.*, vol. 32, no. 2, pp. 376–382, 2004.

[69] W. Seering *et al.*, "The function of the primary ligaments of the knee in varus-valgus and axial rotation," *J. Biomech.*, vol. 13, no. 9, pp. 785–794, 1980.

[70] M. Kersh, "Virtual biomechanical knee: A finite element ligament model with experimental validation," *Ph.D. dissertation, Materials Sci. Eng., Univ. Wisconsin-Madison*, Madison, WI, USA, 2010.

[71] J. L. Haimes *et al.*, "Role of the medial structures in the intact and anterior cruciate ligament-deficient knee. Limits of motion in the human knee," *Amer. J. Sports Med.*, vol. 22, pp. 402–409, 1994.

[72] T. D. MacLeod *et al.*, "Magnetic resonance analysis of loaded meniscus deformation: A novel technique comparing participants with and without radiographic knee osteoarthritis," *Skeletal Radiol.*, vol. 44, no. 1, pp. 125–135, 2015.

[73] B. D. Beynnon and B. C. Fleming, "Anterior cruciate ligament strain in-vivo: A review of previous work," *J. Biomech.*, vol. 31, no. 6, pp. 519–525, 1998.

[74] H. Aagaard and R. Verdonk, "Function of the normal meniscus and consequences of meniscal resection," *Scand. J. Med. Sci. Sports*, vol. 9, no. 3, pp. 134–140, 1999.

[75] K. Messner and J. Gao, "The menisci of the knee joint. Anatomical and functional characteristics, and a rationale for clinical treatment." *J. Anat.*, vol. 193, pp. 161–178, 1998.

[76] K. Shelburne, "Modeling the mechanics of the normal and reconstructed knee," 1996.

[77] C. R. Smith *et al.*, "The influence of component alignment and ligament properties on tibiofemoral contact forces in total knee replacement," *J. Biomech. Eng.*, p. 2016.

[78] C. J. Westphal *et al.*, "Load-dependent variations in knee kinematics measured with dynamic MRI," *J. Biomech.*, vol. 46, no. 12, pp. 2045–2052, 2013.

[79] J. P. Halloran *et al.*, "Adaptive surrogate modeling for efficient coupling of musculoskeletal control and tissue deformation models," *J. Biomech. Eng.*, vol. 131, no. 1, p. 011014, 2009.

[80] G. Glen and K. Isaacs, "Estimating sobol sensitivity indices using correlations," *Environ. Model Softw.*, vol. 37, pp. 157–166, 2012.

[81] P. Hansen *et al.*, "Mechanical properties of the human patellar tendon, in vivo," *Clin. Biomech.*, vol. 21, no. 1, pp. 54–58, 2006.

[82] H. U. Stäubli *et al.*, "Mechanical tensile properties of the quadriceps tendon and patellar ligament in young adults," *Amer. J. Sports Med.*, vol. 27, no. 1, p. 27, 1999.

[83] N. Chandrashekar *et al.*, "Sex-based differences in the tensile properties of the human anterior cruciate ligament," *J. Biomech.*, vol. 39, no. 16, pp. 2943–2950, 2006.

[84] D. L. Butler *et al.*, "Comparison of material properties in fascicle-bone units from human patellar tendon and knee ligaments," *J. Biomech.*, vol. 19, no. , pp. 425–432, 1986.

[85] A. Race and A. A. Amis, "The mechanical properties of the two bundles of the human posterior cruciate ligament," *J. Biomech.*, vol. 27, no. 1, pp. 13–24, 1994.

[86] T. Sugita and A. A. Amis, "Anatomic and biomechanical study of the lateral collateral and popliteofibular ligaments," *Amer. J. Sports Med.*, vol. 29, no. 4, p. 466, 2001.

[87] G. Marinozzi *et al.*, "Human knee ligaments: Mechanical tests and ultra-structural observations," *J. Ortho Traum (It)*, vol. 9, no. 2, p. 231, 1983.

[88] P. S. Trent *et al.*, "Ligament length patterns, strength, and rotational axes of the knee joint," *Clin. Orthop. Relat. Res.*, vol. 117, no. p. 263, 1976.

[89] S. Amiri *et al.*, "Mechanics of the passive knee joint. Part 1: The role of the tibial articular surfaces in guiding the passive motion," *Proc. IMechEngr, Part H: J. Eng. Med.*, vol. 220, no. 8, pp. 813–822, 2006.

[90] L. Blankevoort and R. Huiskes, "Validation of a three-dimensional model of the knee," *J. Biomech.*, vol. 29, no. 7, pp. 955–961, 1996.

[91] K. B. Shelburne and M. G. Pandy, "A musculoskeletal model of the knee for evaluating ligament forces during isometric contractions," *J. Biomech.*, vol. 30, no. 2, pp. 163–176, 1997.

[92] K. B. Shelburne and M. G. Pandy, "A dynamic model of the knee and lower limb for simulating rising movements," *Comput. Meth. Biomech. Biomed. Eng.*, vol. 5, no. 2, pp. 149–160, 2002.

[93] C. S. Shin *et al.*, "The influence of deceleration forces on acl strain during single-leg landing: A simulation study," *J. Biomech.*, vol. 40, no. 5, pp. 1145–1152, 2007.

[94] F. Sheehan and J. E. Drace, "Human patellar tendon strain. A noninvasive, in vivo study," *Clin. Orthop.*, vol. 370, pp. 201–207, 2000.

[95] J. Hashemi *et al.*, "An alternative method of anthropometry of anterior cruciate ligament through 3-d digital image reconstruction," *J. Biomech.*, vol. 38, no. 3, pp. 551–555, 2005.

Authors' photographs and biographies not available at the time of publication.